HFC-134a refrigerant gas hydrate formation process and RIN model

ZHAO Yongli[1,2], GUO Kaihua[2], LIU Xiaocong[2], FAN Shuanshi[2], SHU Bifen[2] & GE Xinshi[1]

1. Department of Thermal Engineering, University of Science and Technology of China, Hefei 430070, China
2. Guangzhou Institute of Energy Conversion, Chinese Academy of Sceinces, Guangzhou 510070, China;

Correspondence should be addressed to Guo Kaihua (e-mail: guokh@ms.gies.ac.cn)

Abstract **In this paper, the macroscopic visualization experiments of HFC-134a refrigerant gas hydrate formation are investigated. According to the macroscopic photos and Mori's microscopic photos of HFC-134a hydrate formation process, the mechanism of gas hydrate formation is analyzed. A random inducement nucleation model is presented to describe the hydrate formation process. The factors affecting the fractal growth dimension in the model, such as step, branch increment and angle, are discussed.**

Keywords: refrigerant gas hydrate, crystallization, formation process photos, RIN model.

Gas hydrate are crystalline compounds that are formed when water and gas or volatile liquid come in contact under conditions of high pressure and low temperature. Hydrates are formed in a highly structured system where all the water molecules are hydrogen bonded in a crystal cavity and the gas molecule dissolves in the cavity and interacts with the water through van der Waals forces. Refrigerant gas hydrates can be effectively formed at appropriate temperature (5℃—12℃) with large reaction heat (320—430 kJ/kg). Because of their particular thermodynamic properties, refrigerant hydrates have been considered as one of the most promising cool storage media for air conditioning systems[1,2]. Natural gas hydrates are being regarded as future potential energy sources because of findings of a great amount of natural gas hydrates in the ocean[3,4]. The formation processes of gas hydrate have become an important and pressing subject in energy and environment research field as well as in natural gas industry.

The formation of gas hydrate takes place in a multiphase (refrigerant gas phase, refrigerant liquid phase, liquid water phase, and solid hydrate phase) system. The gas hydrate formation process is characterized by a low phase-diffusion speed, a long inducement time, a large supercooling, and a low formation rate. Many articles of dynamic research of gas hydrate formation have been found[3—7]. The formation morphology studies are mainly included in Makagon's thesis[4]. Mori[8,9] obtained the HFC-134a hydrate formation process photos but the growth model was not founded. Zhao et al.[10] observed the HCFC-141b hydrate formation process with a microscope.

In agglomeration state physics, fractal and fractal dimension can preferably describe some nonreversible growth process far from the equilibrium state such as phase transition and self-similarity in critical phenomena[11,12]. Applying fractal theory, Min[13] founded the nucleation-limited aggregation model of $BaNO_3$ crystallization growth, and Zhang[14] founded the nucleation aggregation model.

In this paper, a morphology experiment on HFC-134a hydrate formation is reported and a series of macroscopic formation process photos are provided. A model of growth is also proposed according to the fractal theory.

1 Experiment

(ⅰ) Experimental apparatus. The low-temperature visualization experimental system is composed of a test chamber, a cooling system, a heating system, a data acquisition control system, and a digital photo system. The apparatus is shown in fig. 1.

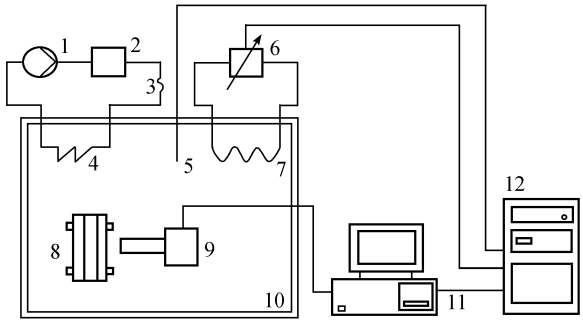

Fig. 1. Schematic of experimental apparatus. 1, Compressor; 2, condenser; 3, capillary; 4, evaporator; 5, thermocouple; 6, thyristor; 7, heater; 8, hydrate reactor; 9, digital video camera; 10, glass chamber; 11, computer; 12, data acquisition and control system.

The test chamber is made of hollow windows to insulate heat from outside. A moisture absorbent is put in the interlayer of the hollow windows to absorb water vapor in the interlayer and to prevent water frost forming inside when temperature becomes low. The cooling system is a small refrigerator. The heating pipe is controlled by a thyristor. In the chamber, six thermocouples were placed to measure the temperature, which was controlled through a HP data acquisition and control system.

A continually focused digital video camera (Panasonic NV-DX100EN) is used to observe the HFC-134a hydrate formation process. The digital photo caught by the camera was input in the computer through a photo acquisition card (DC-30Plus).

(ⅱ) HFC-134a hydrate macroscopic formation photos. The hydrate reactor is cylindrical and has inner volume of 1.5×10^{-5} m^3. The front and back faces of the

reactor are made of two pieces of Plexiglas which were mounted on the stainless steel cylindrical wall with two flanges. The distance between the two pieces of Plexiglas is 6.0×10^{-3} m. Water and HFC-134a were fed into the reactor. Then the reactor was put in the test chamber which had been set at 0.5℃. When the temperature in the reactor was stable, the digital photos system was taken continuously. The formation process photos are shown in fig. 2.

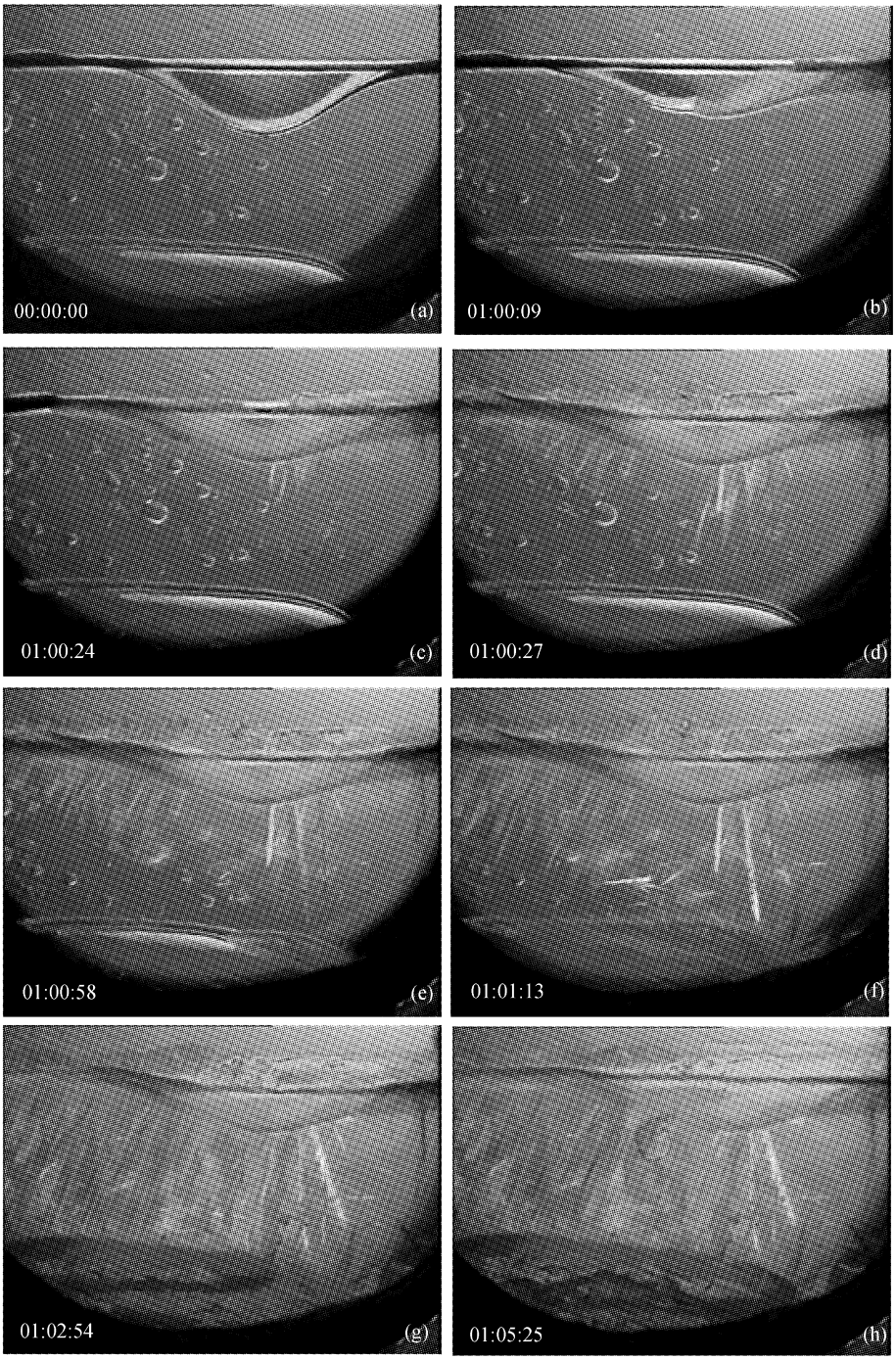

Fig. 2. Morphology of HFC-134a gas hydrate formation process.

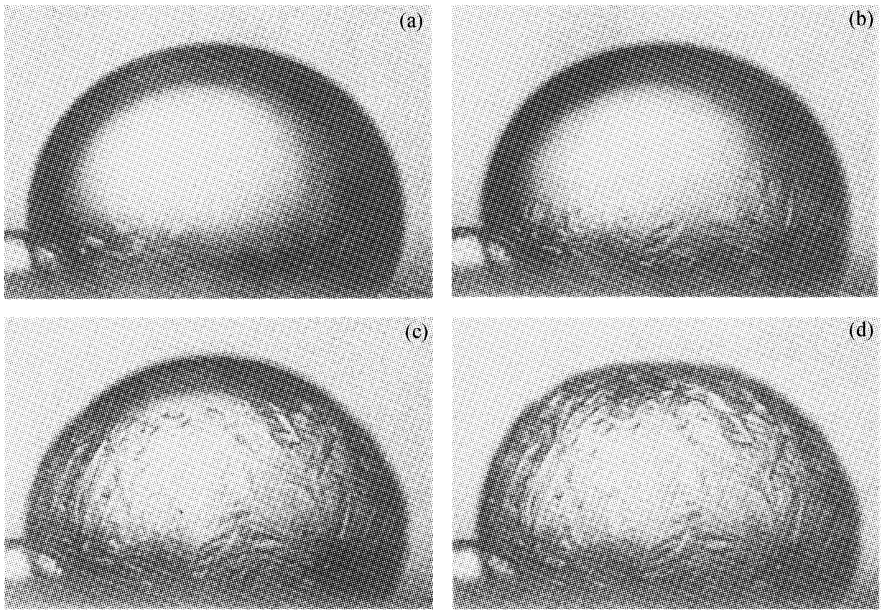

Fig. 3. Morphology of HFC-134a gas hydrate microscopic formation process (×10) (T=(5.2±0.1)℃, p=(0.482±0.011) MPa). (a) t = 0 s; (b) t = 2 s; (c) t = 6 s; (d) t = 11 s.

The liquid density of HFC-134a is 1.294×10^3 kg/m^3 at 0.5℃ and is larger than that of water. Thus, the main amount of HFC-134a liquid was under the water, while a thin layer of HFC-134a was formed on the upper surface of the water due to viscosity and surface tension of the liquid. The initial situation is shown as in fig. 2(a). It can be seen that there are two interfaces between liquid water and liquid HFC-134a formed at upper and bottom of the water, respectively. Water vapor and HFC-134a vapor are mixed in the top of the reactor. In condition of supercooling, the hydrates are formed after about 1-h inducement time. The reaction first takes place at the top interface between water and HFC-134a. The crystal nucleus were firstly formed at the reactor's wall and then induced to the nearby region.

The nucleation process continued and extended to the whole interface. A layer of hydrate was finally formed on the upper interface of HFC-134a and water. At the same time, the hydrate was also formed in the mixed vapor region. Later, the hydrate was formed at the bottom interface between water and HFC-134a. The hydrate crystals then continually grew into the water because HFC-134a diffused into the water through the two hydrate layers. The processes are shown from fig. 2(b) to (h).

(iii) HFC-134a hydrate microscopic formation photos. Mori[9] put a drop of HFC-134a liquid into the water and observed the surface reaction through glass lens. The microscopic formation photos by magnified 10 times are shown in fig. 3.

The hydrate layer was formed at the interface between HFC-134a and water at 5.2℃. Formed crystal nucleus induced the nearby region and the new hydrate was formed as shown in fig. 3(a). After 2 s, the crystal grew along the interface and continually induced other region. The crystal growth is shown in fig. 3(b) and (c). After 11 s, formed hydrate covered the whole liquid HFC-134a surface. Finally, the hydrate stopped forming because the contact between water and HFC-134a was cut off. The final morphology of hydrate formation is shown in fig. 3(d). The HFC-134a hydrate formation appears like arborization. The branch grows from the trunk and forms another trunk. The branch and trunk grow continually. The whole formation process takes on the self-similarity and has fractal growth characteristics.

2 Photo processing

(ⅰ) Photo transforming. The final morphology of hydrate in fig. 3(d) is a gray photo. The gray photo was first transformed to black/white 2-level photo. The black represents hydrate. According to the continuity of hydrate formation, some unclear parts in the photo were refined to form continuous branches and trunks as shown in fig. 4.

3 RIN model

(ⅰ) Particle system. Particle system has been considered as one of most successful methods for generating a simulation pattern of irregular blurry object[12,15]. This method is quite different from other pattern generation systems but very effective for scenery drawing. The scenery is generated by thousands of irregular random-distribution particles which have certain life cycles and various

moving patterns. The particles in the system are moving constantly in random behavior and can disappear when new particles join into the system. The parameters for every movement of the particle are controlled by a random process to keep good randomicity. The particle system is adopted to simulate the model of crystal formation process of HFC-134a gas hydrate.

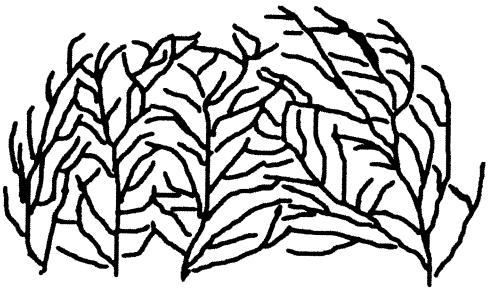

Fig. 4. Black/white schematic (from fig. 3(d)).

(ii) Mechanisms of HFC-134a gas hydrate formation. According to the macroscopic and microscopic formation photos of HFC-134a hydrate, the characteristics of hydrate formation have been detected as in the following:

(1) Gas hydrate can be formed when water and HFC-134a contact in supercooling condition.

(2) Crystal nucleus can occur randomly on the substrate. There appear four seeds of crystal nucleus in fig. 3(b).

(3) Nearby hydrate can be formed by seed stimulation. New hydrate nucleus can be formed and located randomly, but it can be survived only nearby. Because the crystal heat prevents new crystal generation, the new crystallization will be formed away from existing crystal as far as possible，so branches appear. There are two or three branches in fig. 3.

(4) All the seeds will grow up according to the same rule. The nucleus will stimulate and generate the newer continually.

(5) When different branches meet with each other, new nucleus generation will stop.

(6) Finally, the whole surface of the refrigerant liquid droplet is covered by hydrate and stop further growing. The shape of grown crystals has a dendrite pattern.

(iii) RIN Model. The whole hydrate growth process is simulated by the particle system, in which every nucleus is regarded as a particle. The first seed of nucleus is regarded as the seed particle. The seed particle induce the next particle to grow with a certain initial angle and distance. When the second particle is generated, branches will appear randomly near this particle. Then the next branch will be simulated to grow with the same distance and the process goes on generation by generation. The angle has also a random value in a certain range. As time goes by, the second, third, fourth seed will appear soon. Each nucleus grows following the same rule. If two branches meet with each other, they will stop growing. The simulation results are shown in fig. 5. The boundary for this simulation is semicircular. In the program, the initial variables were set before performing the main procedure. Whether the node will grow up is decided by the initial set. If the node can grow, the length of the branch will depend on a random value. The first branch from this node will be regarded as the main stem. The main stem may have a left, a right, both or none branches. This also depends on a random value. With the random angle and the certain length r, the location of the next node can be calculated. A queue is set up in the program for placing the node which will grow next time. The nodes in the queue will grow one by one. The first node in the queue grows first. After the queue finishes from the beginning to the end, the queue will be restarted and repeated until the growth is ended. The node not satisfying the growing condition will disappear in the queue automatically.

(iv) Dimension calculation. The dimensions for scenery presented in fig. 4 and fig. 5(d) are determined with the box counting method. In the program, the number (N) of the black pixel (hydrate) is counted with a circle which has a radius r. Dual logarithm graphics according to r and N are built up. The value of the line slope in the dual logarithm graphics represents the dimension of the scenery. The results are shown in fig. 6. The difference between the two dimension values of the two graphics is very small. Since the real growth of hydrate and the simulation of the growth process are both random processes, the two dimensions will not be exactly the same. It can be seen that the growth dimension varies between 1.69 and 1.85 and the average is 1.78, which is little less than the real growth dimension. Since the growing angles of main stem and branches are random in the simulation, and the earlier contact of adjacent branches and main stem will prevent the part of growth from going on. It can be seen from the simulated graphics that the whole growth is not very even and there are some empty places, which reduce the dimension of simulation.

The growth dimension is synthetically embodied as the structure of hydrate, the speed of growth of hydrate nucleus and the density of hydrate. It is closely related with the outside conditions of the growing process. The parameters used in the program is to meet the outside condition.

(v) Influence of parameters to dimension

(1) Influence of step of main stem or branch. In the simulation, the step is first defined as the number of pixels between one particle and the next. It is the stimulated distance between particles. Under the same outside conditions, the stimulated distance of main stem or branches should be the same. The results of the simulation display

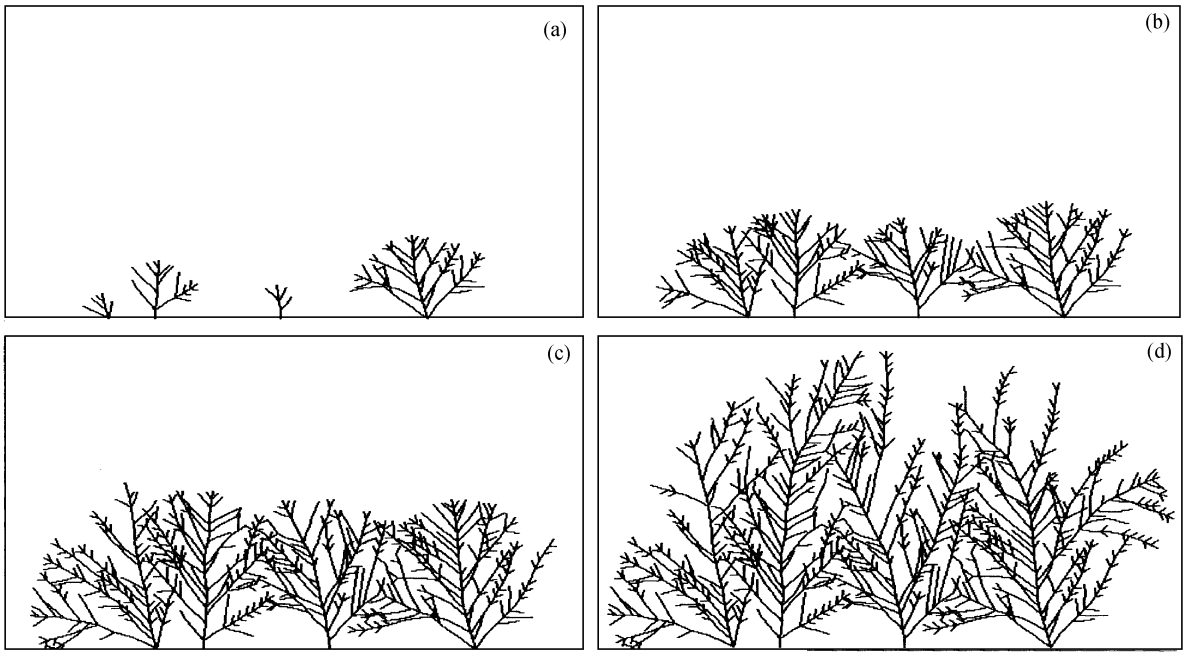

Fig. 5. Schematic of RIN simulation model.

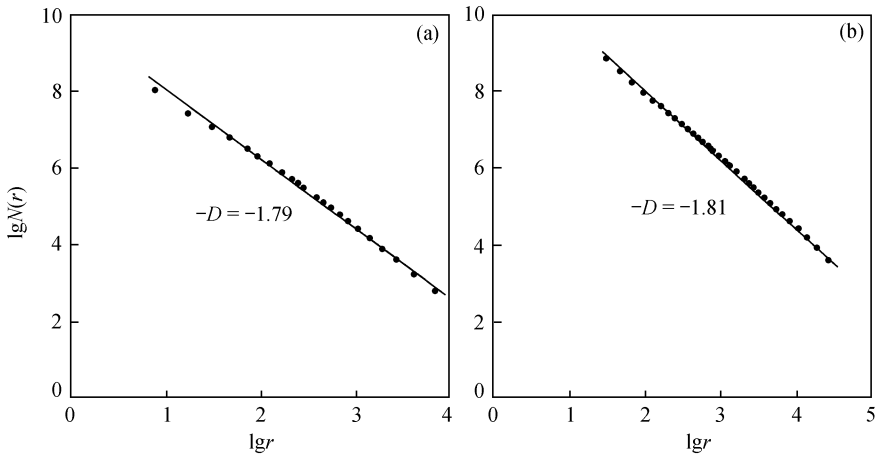

Fig. 6. Dual logarithm graphics for determination of fractal dimension. (a) For scenery of fig. 4; (b) for scenery of fig. 5(d).

that the dimension first increases and then reduces while the step decreases. The increase of the dimension might be due to the dense hydrate branches. Because the number of particles for simulation is limited, when the step is less further, the particles will be exhausted. This results in a large empty space among branches, and the dimension turns small.

(2) Influence of branch increment. In the program, the branch increment for every step in the procedure is specified. The larger this increment is, the faster the branches appear, and the simulated graphics becomes denser. The simulation results show that the more the increment is, the bigger the dimension will be.

(3) Influence of branch angle. The branch angle specified in the program is the upper limitation for variation of the angle between main stem and branches. The angle varing between zero and the branch angle will determine the birth location of the next branch. From the simulation results, it can be seen that the bigger the angle is, the less the dimension is. If the angle is very small, the branches of hydrate will tend to grow in one direction and the hydrate growth becomes denser. When the branch angle is $\pi/4$, hydrate will grow in all directions and appear in disorder.

4 Conclusions

HFC-134a gas hydrate macroscopic formation photos are obtained according to the low temperature viewable crystallization experiment apparatus.

The mechanism of hydrate formation is analyzed. The formation of gas hydrate can be considered as the inducement of nucleation generated in supercooling condition.

A random inducement nucleation model is proposed for fractal pattern simulation. The dimension of the real formation pattern and the simulated pattern are compared. The parameters influencing the growth dimension are also investigated.

Acknowledgements This work was supported by the National Natural Science Foundation of China (Grant Nos. 59836230 and 59706001) and the Major State Basic Research Program (Grant No. G2000026306).

References

1. Guo, K. H., Shu, B. F., Yang, W. J., Advances and application of gas hydrate thermal energy storage technology, Proc. of 1st Trabzon Int. Energy and Environment Symp. (ed. Ayhan, T.), Turkey: Karadeniz Technology University Press, 1996, 1: 381.
2. Guo, K. H., Shu, B. F., Zhang, Y., transient behavior of energy charge-discharge and solid-liquid phase change in mixed gas-hydrate formation, Heat transfer Science and Technology (ed. Wang, B. X.), Beijing: High Education Press, 1996, 728—733.
3. Sloan, E. D., Clathrate Hydrates of Natural Gases, New York: Marcel Dekker, 1997.
4. Makogon, Y. F., Hydrates of Hydrocarbons, Oklahoma: Penny Well books, 1997.
5. James, P. K., Kevin, G. C., Ingrid, L. H. et al., Carbon isotopic evidence for methane hydrate instability during quaternary interstadials, Science, 2000, 288(7): 128.
6. Bishnoi, P. R., Natarajan, N., Kalogerakis, N., A united description of the kinetics of hydrate nucleation, growth and decomposition, Annals of the New York Academy of Science (ed. Sloan, E. D.), 1994, 715: 311.
7. Skovbrog, P., Rasmussen, P., A mass transport limited model for the growth of methane and ethane gas hydrate, Chemical Engineering Science, 1993, 49(17): 1131.
8. Sugaya, M., Mori, Y. H., Behavior of clathrate formation at the boundary of liquid water and fluorocarbon in liquid or vapor state, Chemical Engineering Science, 1996, 51(13): 3505.
9. Mori, Y. H., Mochizuki, T., Mass transport across clathrate hydrate films——A capillary permeation model, Chemical Engineering Science, 1997, 52(20): 3613.
10. Zhao, Y. L., Guo, K. H., Fan, S. S. et al., Microscopic view of refrigerant gas hydrate growth, Journal of Chemical Industry and Engineering (in Chinese), 2000, 54(6): 1.
11. Mandelbrot, B. B., The Fractal Geometry of Nature, San Francisco: Freeman, 1982.
12. Vicsek, T., Fractal Growth Phenomena, Sigapore: World Scientific, 1992.
13. Min, N. B., Wang, M., Peng, R. W., Nucleation-limited aggregation in fractal growth, Physical Rev., 1993, 48(1): 621.
14. Zhang, J. Z., Nucleation aggregation model of fractal growth of molybdenum oxide, Acta Physica Sinica (in Chinese), 1992, 41(8): 1302.
15. Peng, Q. S., Bao, H. J., Jin, X. G., Computer True Picture Arithmetic Base, Beijing; Science Press, 1999.

(Received April 2, 2001)